ACES Asian Chemical Editorial Society

DOI: 10.1002/asia.201600067

CHEMISTRY AN ASIAN JOURNAL Communication

Lithium-Ion Batteries

SPECIAL ISSUE

Nano/Micro-Structured Si/C Anodes with High Initial Coulombic Efficiency in Li-Ion Batteries

Quan Xu,[a, b] Jin-Yi Li,[a, b] Ya-Xia Yin,[a] Yi-Ming Kong,[a] Yu-Guo Guo,*[a, b] and Li-Jun Wan[a]

Abstract: One of the major challenges for designing high-capacity anode materials is to combine both Coulombic efficiency and cycling stability. Herein, nano/micro-structured Si/C composites are designed and synthesized to address this challenge by decreasing the specific surface area and improving the tap density of Si/C materials. An ultrahigh initial Coulombic efficiency of 91.2% could be achieved due to a proper particle size, low specific surface area, and optimized structure. The nano/micro-structured Si/C anodes exhibit excellent cycling stability with 96.5% capacity retention after 100 cycles under a current density of 0.2 $A g^{-1}$.

Lithium-ion batteries (LIBs) have become the most important energy storage system for portable devices and electrical vehicles due to their high energy density and long cycle life.[1–3] Growing demands for high-energy LIBs have aroused extensive interest in developing high-capacity electrode materials.[4–6] Silicon, known for its high lithium-storage capacity, was proposed as the most attractive materials for high-energy LIBs.[7–9] The primary challenge of Si anodes was the huge volume change (~300%) during (de)lithiation process, which caused the pulverization of electrodes and instability of the solid–electrolyte interphase (SEI).[10,11] Decreasing the size of Si to the nanoscale was an effective approach to prevent the pulverization of Si.[12,13] However, nanomaterials also displayed some disadvantages, including surface side reactions, large surface area, and electrochemical agglomeration, which led to low Coulombic efficiency (CE) and severe capacity fading.[14–16]

To address these problems, various Si/C composites were fabricated to enhance the electrochemical performance of Si-based anodes.[17–20] However, it was difficult to combine both Coulombic efficiency and cycling stability.[14] A lower CE, especially initial CE (less than 85%) was often presented in recent reports in which the Si-based composites showed a proper electrochemical performance.[21–23] In this case, a large amount of Li-ions, provided by the cathode, would be consumed in practical applications.[20] In addition, a scalable fabrication process of Si/C composites was still a significant challenge.[4,13] Therefore, successful implementation of Si/C as commercial anode materials has been impeded. Spray drying is an effective method for the transformation of materials from the slurry into dried particulate by spraying the materials into a hot drying medium.[24] Recently, Si/C composites have been fabricated by using an open-air drying system.[25–27] However, nano-Si was easily oxidized, which could lead to poor electrochemical performance. Therefore, a closed cycle system was used to fabricate the Si/C composite under N_2 atmosphere and ethanol solvent in this work. The spray drying process was beneficial to mix materials uniformly and obtain porous structure due to the solvent evaporation.[27] Furthermore, the use of the closed cycle system enabled gas and solvent recovery.

In this study, we synthesized nano/micro-structured Si/C composites by using a closed cycle drying system to improve the CE, especially for the first cycle. With this optimized structure, the surface area of compact Si/C composites decreased to 10.5 $m^2 g^{-1}$, corresponding to a high tap density. The nano/micro-structured Si/C anode also demonstrated proper reversible capacity and excellent capacity retention after 200 cycles.

Concurrent fracture of Si particles and the SEI layer has been identified as the main reasons for the poor electrochemical performance of Si-based materials.[6] It was effective to mitigate mechanical degradation by decreasing the particle size to the nanoscale.[4] Therefore, nano-Si (Figure 1a) was used as starting material in the precursor solution. However, the significant increase of surface area could seriously influence the CE of nano-Si electrodes due to the formation of an unstable SEI layer.[20] Although pioneering works demonstrated that porous Si/C composite microspheres would be the desirable solution to overcome the limitations of nano-Si electrodes, the uniform dispersion of nano-Si and the appropriate surface area of porous Si/C were challenging.[3,27–29] Herein, the nano-Si and flake graphite with different size were used to construct nano/micro-structured Si/C composites (Figure 1). The particle size distribution (PSD) curves (Figure 2a) showed that the raw materials possessed proper particle size distribution, which was essential to establish an engineered structure.

[a] Q. Xu, J.-Y. Li, Dr. Y.-X. Yin, Y.-M. Kong, Prof. Y.-G. Guo, Prof. L.-J. Wan
CAS Key Laboratory of Molecular Nanostructure&Nanotechnology and Beijing National Laboratory for Molecular Sciences
Institute of Chemistry
Chinese Academy of Sciences (CAS)
Beijing, 100190 (P. R. China)
E-mail: ygguo@iccas.ac.cn

[b] Q. Xu, J.-Y. Li, Prof. Y.-G. Guo
University of Chinese Academy of Sciences
Beijing, 100190 (P. R. China)

Supporting information for this article can be found under http://dx.doi.org/10.1002/asia.201600067.

This manuscript is part of a special issue on energy conversion and storage. Click here to see the Table of Contents of the special issue.

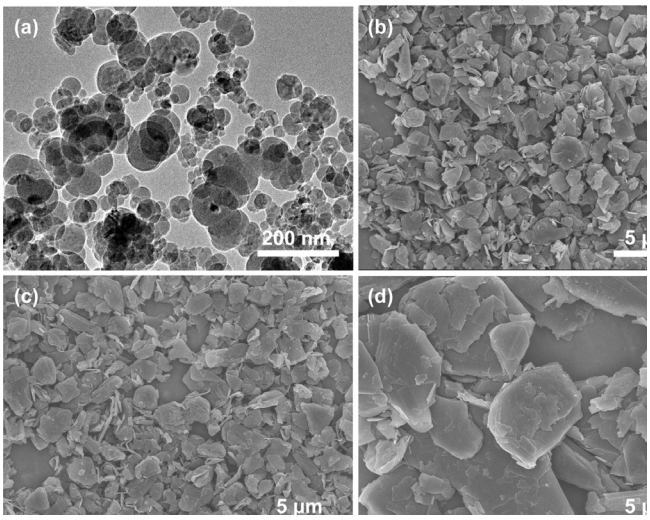

Figure 1. (a) TEM image of nano-Si. SEM images of (b) flake graphite (average diameter = 1 μm), (c) flake graphite (average diameter = 5 μm) and (d) flake graphite (average diameter = 10 μm).

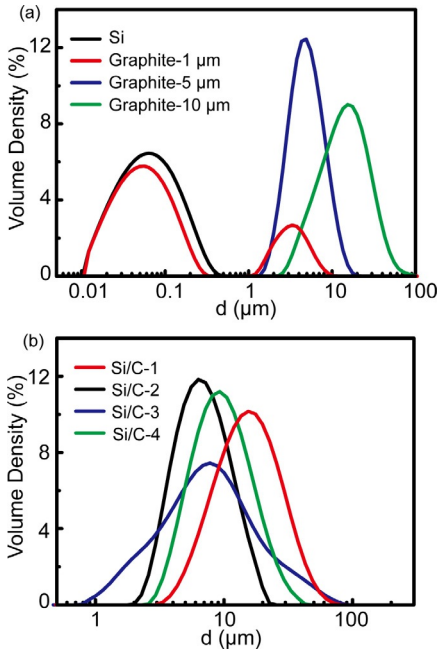

Figure 2. The PSD curves of (a) starting materials and (b) the various Si/C composites obtained by the closed cycle drying system.

The nano/micro-structured Si/C composites were prepared by using a closed cycle drying system, which was reported as high-efficiency method to fabricate porous materials.[24] The existing pores could accommodate the huge volume expansion of nano-Si and allow for the rapid infiltration of electrolyte (Figures S1 and S3). As shown in Figure 2b, the PSD curves of obtained Si/C composites presented a distinct size distribution, consistent with the subsequent analysis by scanning electron microscopy (SEM, see Figure 3), which could be ascribed to the original flake graphite with various average diameter. The size distribution of Si/C-3 was wider than that of other Si/C materials due to the large-sized flake graphite (average diameter = 10 μm), which was difficult to fabricate uniform Si/C composites by closed cycle drying system. Furthermore, Si/C-3 (Figure 3b) was fragile because of a loose structure, leading to a high specific surface area (SSA) of up to 98.2 $m^2 g^{-1}$. Commercial LIBs are mainly based on micro-sized electrodes materials, which limits their structural stability, kinetics and Li-ion intercalation capacities.[2] Si/C-1 (Figure 3d) showed a proper size commonly used in the production of commercial anode materials. It was noted that the average diameter of Si/C composites increased when larger-size flake graphite was used in the slurry. As shown in Figure 3a and 3b, the average diameter of Si/C-2 was only 6.69 μm, but the surface of Si/C-2 was smooth and compact, compared with Si/C-3. The hybrid Si/C-4 (Figure 3c) displayed suitable sphericity and size distribution. Therefore, the optimal Si/C-1 was fabricated by the combination of flake graphite with different average diameter. Diverse size was conducive to efficiently occupy space by filling the interstitial with smaller particles, rather than packing uniform Si/C materials which would leave a large interstitial volume.[13] The obtained Si/C-1 presented a smooth surface, compact structure and superior size distribution, which were beneficial to enhance the electrochemical performance of Si/C anodes with high mass loading.

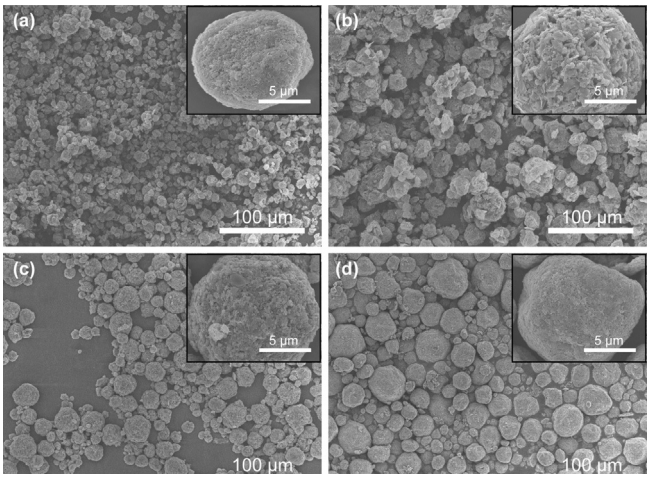

Figure 3. SEM images of (a) Si/C-2, (b) Si/C-3, (c) Si/C-4 and (d) Si/C-1 composites.

The structure of Si/C composites was further characterized by XRD and Raman spectroscopy (Figure 4). The Si/C composites were composed of crystalline Si, graphitic carbon, disordered carbon, and no other impurities were present which could be ascribed to the protection by the inactive atmosphere during spray drying and the calcination process. According to the thermogravimetric analysis (Figure S3), the carbon content of Si/C-1 is approximately 84.5%. The Raman spectrum demonstrated a sharp adsorption peak at around 515 cm^{-1} and two small adsorption peaks at 295 and 950 cm^{-1}, indicating crystalline Si.[19] The other two primary peaks at 1351 and 1601 cm^{-1} correspond to D and G bands, respectively. The ratio of the integrated area of the D and G bands reflects the graphitization degree of the Si/C composites.[21] The low I_D/I_G

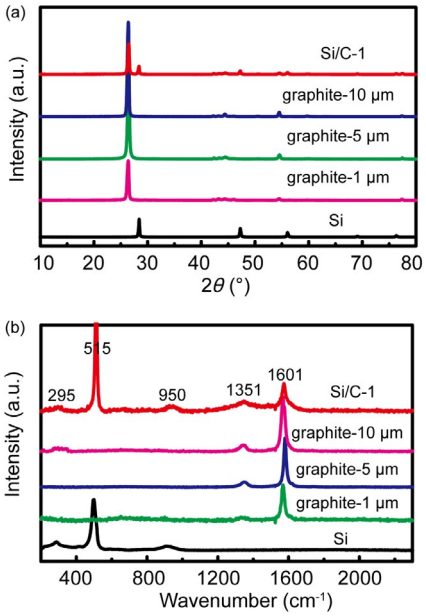

Figure 4. (a) XRD patterns and (b) Raman spectra of various samples.

ratios of the Si/C composites suggest that they had superior electrical conductivity. The conductive framework, which is composed of flake graphite, not only functioned as the electrical highway and mechanical backbone to maintain the structural integrity during cycling but also promoted the formation of a stable SEI layer.

In nano-Si electrodes, the enormously exposed surface resulted in the formation of more interparticle space and the occurrence of severe side reactions which lowered the CE and tap density.[13] As shown in Table 1, the Si/C-1 anode exhibited an ultrahigh initial CE of up to 91.2% which could be attributed to the following aspects: (1) most of the SEI layer formed on the outer surface of Si/C composites instead of nano-Si due to the disordered carbon layer (Figure S2);[17] (2) the nano/micro-structure is favorable for electrolyte penetration, and all nano-Si could participate in the electrochemical reactions;[16] and (3) the lower specific surface area and higher tap density were beneficial to decrease the thickness of electrodes and the distance of the electron pathway under the same mass loading.[4] The average CE of Si/C-1 from the 2nd to the 200th cycle was 99.65% at a relatively slow rate of 0.2 A g^{-1}. However, when the Si/C-1 anode was measured under a constant current of 0.5 A g^{-1}, the average CE of Si/C-1 from the 2nd to the 200th cycle could be increased to 99.8% (Figure S5).

Table 1. Comparison of the properties of Si/C composites.

Samples	Average diameter [μm]	SSA [$m^2 g^{-1}$]	Tap density [$g cm^{-3}$]	Initial CE [%]
Si/C-2	6.69	40.8	0.65	80.3
Si/C-3	8.47	98.2	0.53	76.9
Si/C-4	9.42	22.8	0.72	86.9
Si/C-1	15.3	10.5	0.81	91.2

With well-established Si/C composites built from optimized nano/micro-structure, excellent electrochemical performance could be achieved. Figure 5a shows the first charge and discharge profiles of Si/C anodes at 0.1 A g^{-1} between 1 V and 0.005 V. The Si/C-1 anode demonstrated the highest reversible capacity due to the ultrahigh initial CE, indicating that the novel nano/micro-structure enables the formation of a stable SEI layer during the first cycle.[21] The mass loading of all Si/C anodes were around 3.1 mg cm^{-2} excluding super-P and binder. As shown in Figure 5b, stable cycling of the Si/C-1 anode for 100 cycles with 96.5% capacity retention was achieved under a current density of 0.2 A g^{-1}. Furthermore, it should be noted that the reversible areal capacity reached

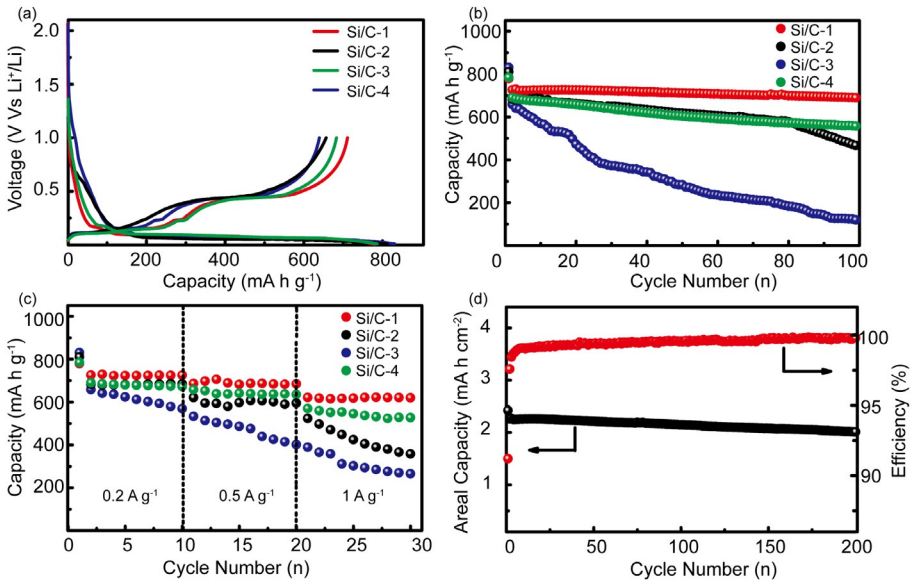

Figure 5. (a) The first charge and discharge profiles. (b) The cycling stability of different Si/C anodes. (c) Rate capability of different Si/C anodes. (d) High areal mass loading test and Coulombic efficiency of the Si/C-1 anode.

2.25 mA h cm^{-2} (Figure 5 d). Even after 200 cycles, the areal capacity was still more than 2 mA h cm^{-2}.

The Si/C-1 anode also displayed a superior rate capability under the same charge/discharge current density (Figure 5 c). About 85.5 % of the original capacity was maintained when the current density was increased from 0.2 A g^{-1} to 1 A g^{-1}. As shown in Figure S5, the Si/C-1 anode also presented proper capacity retention, with 88.5 % of the second discharge capacity after 200 cycles under the current density of 0.5 A g^{-1} (0.7 C). The high CE, associated with the stable SEI layer, contributes to the superior cycling stability. The stable cycling of a high mass loading battery is another advantage of the nano/micro-structured Si/C anodes. There are two interdependent characteristics of the nano/micro-structured design to ensure an excellent performance at high areal capacity. The first is a sufficient and well-established internal void space which is essential to maintain the structural integrity of the Si/C anodes. The second is the carbon framework. It is beneficial to form a stable SEI layer and to obtain electrically connected Si/C materials.

In summary, we synthesized nano/micro-structured Si/C composites by using a closed cycle drying system which exhibited an ultrahigh initial CE of 91.2 % under the current density of 0.1 A g^{-1}. About 88.9 % capacity retention was achieved under a current density of 0.2 A g^{-1} after 200 cycles, even when the reversible areal capacity was up to 2.25 mA h cm^{-2}. Furthermore, the scalability and manufacturing efficiency of Si/C anodes meet the requirements of practical application. The facile fabrication process and superior performance make Si/C anodes a promising alternative to graphite for obtaining LIBs with a high energy density.

Experimental Section

Synthesis

Firstly, 10 g nano-Si, 10 g polyvinyl pyrrolidone and 10 g phenolic resin were stirred in ethanol (600 mL) under sonication for 2 h. Then, 10 g flake graphite (average diameter = 10 μm), 15 g flake graphite (average diameter = 5 μm) and 20 g flake graphite (average diameter = 1 μm) were added to the above solution, followed by vigorous stirring for 12 h to form a homogeneous slurry. The resulting solution was used to prepare Si/C composites by closed cycle drying system under N_2 atmosphere. The obtained Si/C composites were pyrolyzed at 1000 °C for 3 h at a heating rate of 5 °C min^{-1} under argon atmosphere. The obtained Si/C composites were denoted as Si/C-1. For comparison, Si/C-2, Si/C-3 and Si/C-4 were prepared by the same process. However, the flake graphite used was different. The slurry of Si/C-2 was composed of 45 g flake graphite (average diameter = 1 μm). The slurry of Si/C-3 contained 45 g flake graphite (average diameter = 10 μm). For the fabrication of Si/C-4, 19 g flake graphite (average diameter = 5 μm) and 26 g flake graphite (average diameter = 1 μm) were used in the slurry.

Characterization

The morphologies of all materials were investigated by SEM (JEOL 6701F) and TEM (JEM-2100F). X-ray diffraction patterns (XRD) were obtained by using a Rigaku D/max 2500 diffractometer using $Cu_{K\alpha}$ radiation. Particle size distribution (PSD) was measured using a laser particle size analyzer (Malvern, Mastersizer 3000). Raman spectra were obtained using a Digilab FTS3500 spectrophotometer. CR2032-type coin cells were assembled to measure the electrochemical performance in an Ar-filled glove box. The half cells were composed of Li foil as the counter electrode, a Celgard 2500 membrane as separator, the electrolyte and the working electrode. The electrolyte was 1 M $LiPF_6$ in a mixture of ethylene carbonate (EC), dimethyl carbonate (DMC), and diethyl carbonate (DEC) (1:1:1, v/v/v, 70 μL) containing 5 % fluoroethylene carbonate (FEC) and 2 % vinylene carbonate (VC) additives. Si/C composites were mixed with super P, sodium carboxymethyl cellulose (CMC) and styrene butadiene rubber (SBR) in the mass ratio of 90:5:2.5:2.5 to form a homogeneous slurry in deionized water. The obtained slurry was pasted onto the carbon-coated copper and then dried in a vacuum oven at 60 °C for 12 h. The loading of active materials was around 3.1 mg cm^{-2}. The charge and discharge measurements of batteries were carried out in a voltage range of 0.005–1.0 V vs. Li^+/Li under a constant current of 0.1 A g^{-1} for the first cycle and 0.2 A g^{-1} for later cycles.

Acknowledgements

This work was supported by the National Basic Research Program of China (Grant No. 2012CB932900), the National Natural Science Foundation of China (Grant Nos. 51225204, and 21127901), and the "Strategic Priority Research Program" of the Chinese Academy of Sciences (Grant No. XDA09010000) and CAS.

Keywords: anodes · Coulombic efficiency · lithium-ion batteries · nano/micro-structures · Si/C

[1] H. Li, Z. Wang, L. Chen, X. Huang, *Adv. Mater.* **2009**, *21*, 4593 – 4607.
[2] Y. G. Guo, J. S. Hu, L. J. Wan, *Adv. Mater.* **2008**, *20*, 2878 – 2887.
[3] A. Magasinski, P. Dixon, B. Hertzberg, A. Kvit, J. Ayala, G. Yushin, *Nat. Mater.* **2010**, *9*, 353 – 358.
[4] X. Li, M. Gu, S. Hu, R. Kennard, P. Yan, X. Chen, C. Wang, M. J. Sailor, J. G. Zhang, J. Liu, *Nat. Commun.* **2014**, *5*, 4105.
[5] X. L. Wu, Y. G. Guo, L. J. Wan, *Chem. Asian J.* **2013**, *8*, 1948 – 1958.
[6] Q. Zhang, X. Xiao, W. Zhou, Y. T. Cheng, M. W. Verbrugge, *Adv. Energy Mater.* **2015**, *5*, 1401398.
[7] J. Chang, X. Huang, G. Zhou, S. Cui, P. B. Hallac, J. Jiang, P. T. Hurley, J. Chen, *Adv. Mater.* **2014**, *26*, 758 – 764.
[8] Y. Du, G. Zhu, K. Wang, Y. Wang, C. Wang, Y. Xia, *Electrochem. Commun.* **2013**, *36*, 107 – 110.
[9] C. K. Chan, H. Peng, G. Liu, K. McIlwrath, X. F. Zhang, R. A. Huggins, Y. Cui, *Nat. Nanotechnol.* **2008**, *3*, 31 – 35.
[10] X. Xiao, W. Zhou, Y. Kim, I. Ryu, M. Gu, C. Wang, G. Liu, Z. Liu, H. Gao, *Adv. Funct. Mater.* **2015**, *25*, 1426 – 1433.
[11] J. S. Kim, W. Pfleging, R. Kohler, H. J. Seifert, T. Y. Kim, D. Byun, H. G. Jung, W. Choi, J. K. Lee, *J. Power Sources* **2015**, *279*, 13 – 20.
[12] J. Song, S. Chen, M. Zhou, T. Xu, D. Lv, M. L. Gordin, T. Long, M. Melnyk, D. H. Wang, *J. Mater. Chem. A* **2014**, *2*, 1257 – 1262.
[13] D. Lin, Z. Lu, P.-C. Hsu, H. R. Lee, N. Liu, J. Zhao, H. Wang, C. Liu, Y. Cui, *Energy Environ. Sci.* **2015**, *8*, 2371 – 2376.
[14] S. H. Ng, J. Wang, D. Wexler, K. Konstantinov, Z. P. Guo, H. K. Liu, *Angew. Chem. Int. Ed.* **2006**, *45*, 6896 – 6899; *Angew. Chem.* **2006**, *118*, 7050 – 7053.
[15] S. J. Kim, M. Naguib, M. Zhao, C. Zhang, H. T. Jung, M. W. Barsoum, Y. Gogotsi, *Electrochim. Acta* **2015**, *163*, 246 – 251.
[16] C. Zhang, Z. Lin, Z. Yang, D. Xiao, P. Hu, H. Xu, Y. Duan, S. Pang, L. Gu, G. Cui, *Chem. Mater.* **2015**, *27*, 2189 – 2194.
[17] N. Liu, Z. Lu, J. Zhao, M. T. McDowell, H. W. Lee, W. Zhao, Y. Cui, *Nat. Nanotechnol.* **2014**, *9*, 187 – 192.

[18] X. Gao, J. Li, Y. Xie, D. Guan, C. Yuan, *ACS Appl. Mater. Interfaces* **2015**, *7*, 7855 – 7862.
[19] S. O. Kim, A. Manthiram, *J. Mater. Chem. A* **2015**, *3*, 2399 – 2406.
[20] Y. He, X. Yu, Y. Wang, H. Li, X. Huang, *Adv. Mater.* **2011**, *23*, 4938 – 4941.
[21] M. Li, X. Hou, Y. Sha, J. Wang, S. Hu, X. Liu, Z. Shao, *J. Power Sources* **2014**, *248*, 721 – 728.
[22] H. Zhang, X. Qin, J. Wu, Y. B. He, H. Du, B. Li, F. Kang, *J. Mater. Chem. A* **2015**, *3*, 7112 – 7120.
[23] X. Zhou, Y. G. Guo, *J. Mater. Chem. A* **2013**, *1*, 9019 – 9023.
[24] K. Cal, K. Sollohub, *J. Pharm. Sci.* **2010**, *99*, 575 – 586.
[25] S. Li, X. Qin, H. Zhang, J. Wu, Y. B. He, B. Li, F. Kang, *Electrochem. Commun.* **2014**, *49*, 98 – 102.
[26] W. Ren, Z. Zhang, Y. Wang, Q. Tan, Z. Zhong, F. Su, *J. Mater. Chem. A* **2015**, *3*, 5859 – 5865.
[27] D. S. Jung, T. H. Hwang, S. B. Park, J. W. Choi, *Nano Lett.* **2013**, *13*, 2092 – 2097.
[28] R. Yi, J. Zai, F. Dai, M. L. Gordin, D. H. Wang, *Nano energy* **2014**, *6*, 211 – 218.
[29] R. Yi, F. Dai, M. L. Gordin, S. Chen, D. H. Wang, *Adv. Energy Mater.* **2013**, *3*, 295 – 300.

Manuscript received: January 18, 2016
Accepted Article published: February 8, 2016
Final Article published: February 23, 2016